

We are IntechOpen, the world's leading publisher of Open Access books Built by scientists, for scientists

6,900

Open access books available

186,000

International authors and editors

200M

Downloads

Our authors are among the

154

Countries delivered to

TOP 1%

most cited scientists

12.2%

Contributors from top 500 universities



WEB OF SCIENCE™

Selection of our books indexed in the Book Citation Index
in Web of Science™ Core Collection (BKCI)

Interested in publishing with us?
Contact book.department@intechopen.com

Numbers displayed above are based on latest data collected.
For more information visit www.intechopen.com



The Effect of the Time Structure of Laser Pulse on Temperature Distribution and Thermal Stresses in Homogeneous Body with Coating

Aleksander Yevtushenko¹ and Malgorzata Rozniakowska-Klosinska²

¹*Bialystok University of Technology*

²*Technical University of Lodz
Poland*

1. Introduction

The need of increased precision and efficiency of thermal processing of modern construction materials with the aid of lasers, makes it especially timely to examine the problem of nonstationary temperature fields in non-homogeneous materials during the heating and cooling stages. This is the reason of continuous interest of many researchers (Kim et al., 1997; Loze & Wright, 1997; Said-Galiyev & Nikitin, 1993; Sheng & Chrysosolouris, 1995).

Providing an example, such materials applied among other things in automotive and power industry, are these in the electrical steel – insulator's layer systems of which transformers' core or magnetic cores in electric engines are made. However, the core-loss occurs as a result of the overheating of these materials due to Joule's effect, this is the reason why the efficiency reduces in electrical devices. The induction currents, which are generated by changing magnetic field and connected with them magnetic structure domains has great influence on transformers' efficiency, too. It turns, that in order to decrease the transformer's core-loss, the size of magnetic structure domains should be decreased. This can be achieved by the application of pulsed laser heating of sheet steel (electrical steel – insulator's layer system), in such manner that homogeneous and stable stresses are made – it is a refinement method of magnetic structure domains. As a final result, a sheet steel with an energy lost of about 10% lower than for conventional sheet steel, is obtained. It should be underlined, that during the induce processing of stresses (setting the desired magnetic domains size) coating should not be damaged, the application of pulsed laser radiation satisfies this condition (Coutouly et al., 1999; Li et al., 1997).

Cleavage of the material in the process of thermal splitting results from tensile stresses when the sample is heated by the moving heat flux. When the stresses value exceeds the tensile strength of material then cracks arise on the surface of the processed sample and they follow the movements of the heat source. The cracks in the material are generated on condition that the temperature is higher than material's temperature corresponding to the thermal strength. But for the purpose of guaranteed destruction of the sample considerable temperature gradient must be produced by heating the smallest possible area. For this reason the heating should proceed quickly, in the pulsed mode and the maximum

temperature should not exceed the temperature of melting for in such conditions the stress quickly disappears. Thermal splitting of brittle non-metals (like glass, ceramic materials, granite) is the easiest of all for they exhibit big difference between the melting temperature and the temperature of thermal strength. Low thermal conductivity of brittle materials is the cause why considerable thermal stresses are generated in thin subsurface layer in the initial moment. As a result, destruction of the sample takes place shortly after the heating process starts.

Laser treatment is one of the methods of improving the properties of coatings. It is applied when the heating of large areas is difficult or when heating should be limited to some specified parts of the product. Ceramic with zirconium dioxide ZrO_2 as a base constituent is one of the most promising materials for thermally insulating coatings (Dostanko et al., 2002). Functional parameters of such coatings can be improved by laser processing. As results the bigger density and smaller porosity are obtained. At the same time a specific structure of the processed surface is formed – many, nearly equidistant micro cracks arose on it. Usually the width of these micro cracks does not exceed 2 μm , the depth – 10 μm and the maximum length of this specific structure of the processed surface is smaller than 50 μm . When the surface with such a layer produced on it undergoes heating, the parts of the coating between micro cracks can slightly change their relative positions what retards the development of destructive macro cracks. This explains experimentally observed thermal strength increase of the zirconium dioxide ZrO_2 coatings after their laser processing (Dostanko et al., 2002).

Ornaments from granite in buildings like churches, theatres and hotels are often covered, to make them more attractive, with thin metallic foil (gold, platinum, copper). Remaining for years in polluted atmospheric air, sooner or later such ornaments require cleaning. Nowadays laser methods are used for this purpose. In the course of the process of cleaning the metallic foil can not be melted and must stay in thermal contact with the substrate. That is the cause why the problem of modelling temperature and stress fields generated by pulsed laser irradiation is so important for the system consisted of a bulk substrate of low thermal conductivity and a thin metallic coating deposited on it.

Analytical methods for calculation of the temperature fields generated by the pulse laser irradiation were developed mainly for homogeneous materials (Duley, 1976; Rykalin et al., 1985; Ready, 1971; Welch & Van Gemert, 1995; Hector & Hetnarski, 1996). On the other hand, the material to be split quite often has the form of a protective coating or thin film deposited on the homogeneous substrate. The mathematical model of controlled thermal splitting of homogeneous and piece-wise homogeneous bodies at assumption of uniform distribution of the heat flux intensity was considered earlier (Li et al., 1997; Yevtushenko et al., 2005). The reviews of different methods of analysis for the thermal phenomena connected with laser heating are presented in the relevant literature (Gureev, 1983; Rozniakowska & Yevtushenko, 2005).

Therefore, the aim of this chapter of the book is the analysis of temperature distribution and thermal stresses in the non-uniform body heated by the heat flow changing in time. For this purpose the analytical solution of the transient heat conduction problem and corresponding thermoelasticity quasi-static problem for the system, which consists of semi-infinite homogeneous substrate with coating and heated by the laser pulse with rectangular or triangular time shape, was used. The obtained solution determines the temperature and thermal stresses in the piecewise homogeneous body both in the heating phase at laser pulse irradiation and in the cooling phase, when the laser is switched off.

2. Temperature field

For small values of Fourier’s numbers, which correspond to characteristic times of thermal splitting, the large part of the heat flux is directed into the body, perpendicularly to its surface. That makes it possible to consider the generation of temperature fields and thermal stresses as the one-dimensional non-stationary process. Let us consider the system of semi-infinite substrate with the coating of the thickness d (Fig. 1). Thermophysical properties of the substrate and the coating differ.

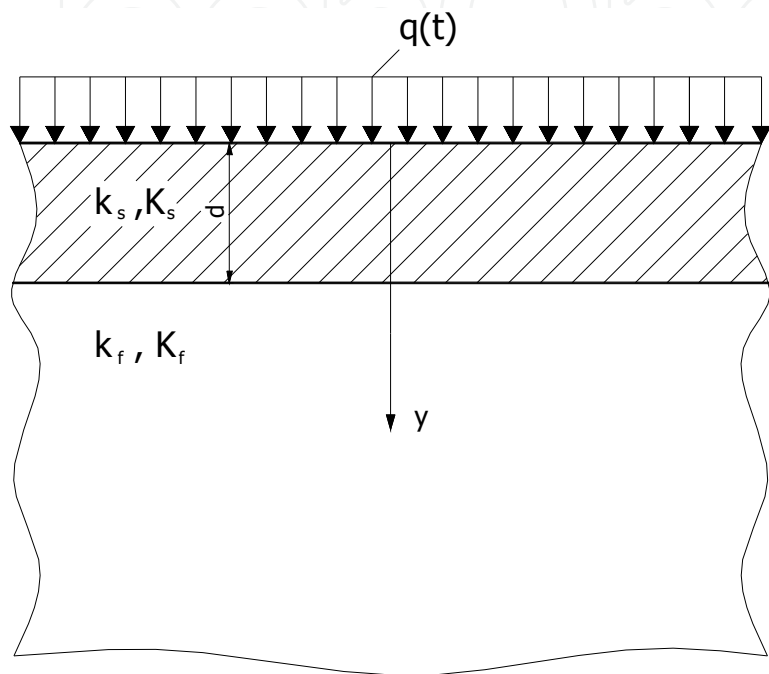


Fig. 1. Heating model of the homogeneous body with coating.

It is assumed, that the intensity of heat flux propagating in the coating material has the following form:

$$q(t) = Aq_0q^*(t), \tag{1}$$

where A is the absorption coefficient, q_0 is the characteristic value of heat flux intensity, t is the time. Usually one assumes a rectangular laser pulse shape

$$q^*(t) = \begin{cases} 1, & 0 < t \leq t_s, \\ 0, & t > t_s, \end{cases} \tag{2}$$

or triangular one with respect to time

$$q^*(t) = \begin{cases} 2t / t_r, & 0 < t \leq t_r, \\ 2(t_s - t) / (t_s - t_r), & t_r \leq t \leq t_s, \\ 0, & t > t_s, \end{cases} \tag{3}$$

where t_r is the pulse rise time, t_s is the laser pulse duration. For comparative numerical analysis the parameters of functions (2) and (3) are chosen in such a manner that pulse

duration and energy are the same in both cases. The perfect thermal contact between the substrate and the coating is assumed. All the values and parameters which refer to coating and the substrate in the further considerations will have bottom indexes c and s respectively. The dimensionless temperature distribution in the coating and in the substrate can be found from the solution of the following boundary-value problem of heat conduction:

$$\frac{\partial^2 T_c^*(\zeta, \tau)}{\partial \zeta^2} = \frac{\partial T_c^*(\zeta, \tau)}{\partial \tau}, \quad 0 < \zeta < 1, \tau > 0, \quad (4)$$

$$\frac{\partial^2 T_s^*(\zeta, \tau)}{\partial \zeta^2} = \frac{1}{k^*} \frac{\partial T_s^*(\zeta, \tau)}{\partial \tau}, \quad 1 < \zeta < \infty, \tau > 0, \quad (5)$$

$$\left. \frac{\partial T_c^*}{\partial \zeta} \right|_{\zeta=0} = -q^*(\tau), \quad \tau > 0, \quad (6)$$

$$T_c^*(1, \tau) = T_s^*(1, \tau), \quad \tau > 0, \quad (7)$$

$$\left. \frac{\partial T_c^*}{\partial \zeta} \right|_{\zeta=1} = K^* \left. \frac{\partial T_s^*}{\partial \zeta} \right|_{\zeta=1}, \quad \tau > 0, \quad (8)$$

$$T_s^*(\zeta, \tau) \rightarrow 0, \quad \zeta \rightarrow \infty, \tau > 0, \quad (9)$$

$$T_c^*(\zeta, 0) = 0, \quad 0 \leq \zeta \leq 1, \quad (10)$$

$$T_s^*(\zeta, 0) = 0, \quad 1 \leq \zeta < \infty. \quad (11)$$

where

$$\zeta = \frac{z}{d}, \quad \tau = \frac{k_c t}{d^2}, \quad K^* = \frac{K_s}{K_c}, \quad k^* = \frac{k_s}{k_c}, \quad T_c^* = \frac{T_c}{T_0}, \quad T_s^* = \frac{T_s}{T_0}, \quad T_0 = A \frac{q_0 d}{K_c}, \quad (12)$$

K, k are coefficients of thermal conductivity and thermal diffusivity, respectively. Taking the equations (2) and (1) into account, the dimensionless temporal profile $q^*(\tau)$ of the laser pulse in the right side of the boundary condition (6) can be written in the form

$$q^*(\tau) = H(\tau_s - \tau), \quad \tau > 0, \quad (13)$$

or

$$q^*(\tau) = \begin{cases} 2\tau / \tau_r, & 0 < \tau \leq \tau_r, \\ 2(\tau_s - \tau) / (\tau_s - \tau_r), & \tau_r \leq \tau \leq \tau_s, \\ 0, & \tau > \tau_s, \end{cases} \quad (14)$$

where

$$\tau_r = \frac{k_c t_r}{d^2}, \quad \tau_s = \frac{k_c t_s}{d^2}, \quad (15)$$

$H(\cdot)$ is the Heaviside's step function.

Solution of a boundary-value problem of heat conduction in friction (4)-(11) by applying the Laplace integral transform with respect to dimensionless time τ

$$L[T_{c,s}^*(\zeta, \tau); p] \equiv \bar{T}_{c,s}^*(\zeta, p) = \int_0^\infty T_{c,s}^*(\zeta, \tau) \exp(-p\tau) d\tau, \quad (16)$$

has form

$$\bar{T}_{c,s}^*(\zeta, p) = \bar{q}^*(p) \frac{\Delta_{c,s}(\zeta, p)}{\sqrt{p} \Delta(p)}, \quad (17)$$

where

$$\Delta_c(\zeta, p) = \text{ch}[(1-\zeta)\sqrt{p}] + \varepsilon \text{sh}[(1-\zeta)\sqrt{p}], \quad 0 \leq \zeta \leq 1, \quad (18)$$

$$\Delta_s(\zeta, p) = \exp\left[-(1-\zeta)\sqrt{\frac{p}{k^*}}\right], \quad \infty < \zeta \leq 1, \quad (19)$$

$$\Delta(p) = \text{sh}\sqrt{p} + \varepsilon \text{ch}\sqrt{p}, \quad (20)$$

$\bar{q}^*(p)$ is the Laplace transform of dimensionless temporal profile $q^*(\tau)$ of the laser pulse, $\varepsilon = K^* / \sqrt{k^*}$ is known as the "thermal activity coefficient of the substrate in relation to the coating" (Luikov, 1986). Taking the expansion into account

$$\frac{1}{1 - \lambda \exp(-2\sqrt{p})} = \sum_{n=0}^{\infty} \Lambda^n \exp(-2\sqrt{p}), \quad (21)$$

where

$$\Lambda^n = \begin{cases} (-1)^n |\lambda|^n, & -1 < \lambda \leq 0, \\ \lambda^n, & 0 \leq \lambda < 1, \end{cases}, \quad \lambda = \frac{1-\varepsilon}{1+\varepsilon}, \quad (22)$$

the transforms (17)-(20) for the temperatures of the coating and substrate can be written as follows

$$\bar{T}_c^*(\zeta, p) = \frac{\bar{q}(p)}{\sqrt{p}} \left\{ \sum_{n=0}^{\infty} \Lambda^n \exp[-(2n+\zeta)\sqrt{p}] + \sum_{n=1}^{\infty} \Lambda^n \exp[-(2n-\zeta)\sqrt{p}] \right\}, \quad 0 \leq \zeta \leq 1, \quad (23)$$

$$\bar{T}_s^*(\zeta, p) = \frac{2\bar{q}(p)}{(1+\varepsilon)\sqrt{p}} \sum_{n=0}^{\infty} \Lambda^n \exp\left\{-\left[(2n+1)\sqrt{p} + (\zeta-1)\sqrt{\frac{p}{k^*}}\right]\right\}, \quad \infty < \zeta \leq 1. \quad (24)$$

The transforms (23) and (24) were obtained for arbitrary form of the function $q^*(\tau)$. Transition into the originals of integral Laplace transform will be at first considered for two

special cases of laser pulses: with constant intensity $q_0^*(\tau) = 1, \tau > 0$ and linearly changing $q_1^*(\tau) = \tau, \tau > 0$. Then, the corresponding Laplace transforms are (Luikov, 1986)

$$\bar{q}_i^*(p) = p^{-1-i}, i = 0, 1. \quad (25)$$

Inversion of formulas (23) and (24) will be conducted independently for the transforms $\bar{q}_0^*(p)$ and $\bar{q}_1^*(p)$ (25) with the use of the convolution theorem for the integral Laplace transform (Luikov, 1986)

$$U_i(\tau) \equiv L^{-1}[\bar{q}_i^*(p)\bar{Q}(p); \tau] = \int_0^\tau q_i^*(s)Q(\tau-s)ds, \tau > 0, i = 0, 1, \quad (26)$$

where

$$\bar{Q}(p) = \frac{\exp(-\sqrt{ap})}{\sqrt{p}}, Q(\tau) = \frac{1}{\sqrt{\pi\tau}} \exp\left(-\frac{a}{4\sqrt{\tau}}\right), \tau > 0, a \geq 0. \quad (27)$$

Then, substitution of the functions $q_i^*(\tau) = 1, i = 0, 1$ and $Q(\tau)$ (27) into right side of the formula (26) gives:

$$U_i(\tau) = \frac{1}{\sqrt{\pi}} \int_0^\tau \frac{s^i}{\sqrt{\tau-s}} \exp\left(-\frac{a}{4\sqrt{\tau-s}}\right) ds, \tau > 0, i = 0, 1. \quad (28)$$

To calculate the integrals (28), a new variable

$$r = \frac{a}{4(\tau-s)}, w = \frac{1}{2}\sqrt{\frac{a}{\tau}}, \tau > 0, \quad (29)$$

is introduced. Then we find

$$U_0(\tau) = \frac{1}{2}\sqrt{\frac{a}{\pi}}u_0(w), U_1(\tau) = \frac{1}{2}\sqrt{\frac{a}{\pi}}\left[\tau u_0(w) - \frac{a}{4}u_1(w)\right], \quad (30)$$

where

$$u_i(w) = \int_{w^2}^\infty \frac{\exp(-r)}{r^{i+1}\sqrt{r}} dr, i = 0, 1. \quad (31)$$

Integration by parts of (31) gives

$$u_0(w) = 2\sqrt{\pi} w^{-1} \text{ierfc}(w), u_1(w) = \frac{2}{3} \left[w^{-3} \exp(-w^2) - u_0(w) \right] \quad (32)$$

where

$$\text{ierfc}(w) = \pi^{-1/2} \exp(-w^2) - w \text{erfc}(w), \text{erfc}(w) = 1 - \text{erf}(w), \quad (33)$$

$\text{erf}(x)$ is Gauss error function. After substitution of functions $u_i(w), i = 0, 1$ (32) into formulas (30) is obtained finally

$$U_i(\tau) = 2\tau^i \sqrt{\tau} F_i(w), \quad i = 0, 1, \quad (34)$$

where

$$F_0(x) = \text{ierfc}(x), \quad F_1(x) = \frac{1}{3} [2(1+x^2)F^{(0)}(x) - x \text{erfc}(x)]. \quad (35)$$

Taking into account the form of functions $U_i(\tau)$, $i = 0, 1$ (34), from the formulas (23) and (24) the dimensionless temperatures $T^{(i)*}$, $i = 0, 1$ are found for the constant $q_0^*(\tau) = 1$ and linearly changing with time $q_1^*(\tau) = \tau$, $\tau > 0$ heat flux intensity, respectively

$$T_c^{(i)*}(\zeta, \tau) = \sum_{n=0}^{\infty} \Lambda^n T_{c,n}^{(i)*}(\zeta, \tau), \quad 0 \leq \zeta \leq 1, \tau \geq 0, \quad i = 0, 1, \quad (36)$$

$$T_s^{(i)*}(\zeta, \tau) = \sum_{n=0}^{\infty} \Lambda^n T_{s,n}^{(i)*}(\zeta, \tau), \quad 1 \leq \zeta < \infty, \tau \geq 0, \quad i = 0, 1, \quad (37)$$

where

$$T_{c,0}^{(i)*}(\zeta, \tau) = 2\tau^{i+1/2} F_i\left(\frac{\zeta}{2\sqrt{\tau}}\right), \quad i = 0, 1, \quad (38)$$

$$T_{c,n}^{(i)*}(\zeta, \tau) = 2\tau^{i+1/2} \left[F_i\left(\frac{2n+\zeta}{2\sqrt{\tau}}\right) + F_i\left(\frac{2n-\zeta}{2\sqrt{\tau}}\right) \right], \quad i = 0, 1; \quad n = 1, 2, \dots, \quad (39)$$

$$T_{s,n}^{(i)*}(\zeta, \tau) = \frac{4\tau^{i+1/2}}{(1+\varepsilon)} F_i\left(\frac{2n+1}{2\sqrt{\tau}} + \frac{\zeta-1}{2\sqrt{k^*\tau}}\right), \quad i = 0, 1; \quad n = 0, 1, 2, \dots \quad (40)$$

Subsequently, when the temperature fields $T_{c,s}^{(i)*}(\zeta, \tau)$, $i = 0, 1$ (36)-(40) are determined then temperature of the non-homogeneous body can be found from the expressions (Yevtushenko et al., 2007)

$$T_{c,s}^*(\zeta, \tau) = T_{c,s}^{(0)*}(\zeta, \tau) - T_{c,s}^{(0)*}(\zeta, \tau - \tau_s) H(\tau - \tau_s), \quad \zeta \geq 0, \tau \geq 0, \quad (41)$$

for the rectangular laser pulse (13) and

$$T_{c,s}^*(\zeta, \tau) = \frac{2}{\tau_r} \left[T_{c,s}^{(1)*}(\zeta, \tau) - T_{c,s}^{(1)*}(\zeta, \tau - \tau_r) H(\tau - \tau_r) \right] - \frac{2}{\tau_s - \tau_r} \left[T_{c,s}^{(1)*}(\zeta, \tau - \tau_r) H(\tau - \tau_r) - T_{c,s}^{(1)*}(\zeta, \tau - \tau_s) H(\tau - \tau_s) \right], \quad \zeta \geq 0, \tau \geq 0, \quad (42)$$

for the triangular one (14).

It must be noted that equations (41) and (42) determine the temperature of the body (composed of coating and substrate) in a point beneath the heated surface ($\zeta \geq 0$), after time $\tau \geq 0$ from the beginning of laser irradiation to the moment, when the cooling of the body is completed. The solutions of the corresponding problems of heat conduction for homogeneous semi-space it is possible to obtain from the first component of the expressions (36) and (37) (for $n = 0$) (Rozniakowska & Yevtushenko, 2005).

Taking the notation (12) into account, the temperature distributions in the coating and substrate write in the form

$$T_{c,s}(z,t) = T_0 T_{c,s}^*(\zeta, \tau), \quad \zeta \geq 0, \quad \tau \geq 0, \quad (43)$$

where the dimensionless functions $T_{c,s}^*(\zeta, \tau)$ have the form (41) or (42).

3. Stresses and deformations

Experimental examinations of the controlled superficial splitting proved that from the three normal components of the stress tensor – longitudinal, lateral and in the direction of heating – only the lateral component σ_y is useful in thermal splitting (Dostanko et al., 2002). As the result of action of this component, thermal splitting proceeds in the direction of the heat flux movement trajectory. The longitudinal component σ_x is undesirable because at its enough greater values exceeding tensile strength of materials, the micro cracks oriented at various angles to the direction of splitting are created and divergence between the line of splitting and the direction of heat flow movement occurs. The normal component of stress tensor σ_z has no essential meaning in one-dimensional problem.

On the basis of these data quasi-static normal stresses σ_y in the coating induced by the non-stationary temperature field (36)-(40) can be determined from the equations, which describe thermal bending of thick plate of the thickness d with free ends (Timoshenko & Goodier, 1951):

$$\sigma_y(z,t) = \sigma_0 \sigma_y^*(\zeta, \tau), \quad 0 \leq z \leq d, \quad t \geq 0, \quad (44)$$

where

$$\sigma_y^*(\zeta, \tau) = \varepsilon_y^*(\zeta, \tau) - T_c^*(\zeta, \tau), \quad 0 \leq \zeta \leq 1, \quad \tau \geq 0, \quad (45)$$

$$\varepsilon_y^*(\zeta, \tau) = \int_0^1 T_c^*(\zeta, \tau) d\zeta + 12(\zeta - 0.5) \int_0^1 (\zeta - 0.5) T_c^*(\zeta, \tau) d\zeta, \quad 0 \leq \zeta \leq 1, \quad \tau \geq 0, \quad (46)$$

$\sigma_0 = \alpha_c E_c T_0 / (1 - \nu_c)$ is the stress scaling factor, α_c is the linear thermal expansion coefficient, E_c is the Young's modulus, ν_c is the Poisson's ratio of the coating material, $T_c^*(\zeta, \tau)$ is the dimensionless temperature field in the coating (41) or (42). When the heating of the plate's surface is realised with the uniform heat flux (2), (13) then the dimensionless lateral deformation ε_y^* (46) can be found from the equation (Yevtushenko et al., 2007):

$$\varepsilon_y^*(\zeta, \tau) = \varepsilon_y^{(0)*}(\zeta, \tau) - \varepsilon_y^{(0)*}(\zeta, \tau - \tau_s) H(\tau - \tau_s), \quad 0 \leq \zeta \leq 1, \quad \tau \geq 0, \quad (47)$$

and for the triangular time shape of the heat pulse (3), (14) one has:

$$\begin{aligned} \varepsilon_y^*(\zeta, \tau) = & \frac{2}{\tau_r} \left[\varepsilon_y^{(1)*}(\zeta, \tau) - \varepsilon_y^{(1)*}(\zeta, \tau - \tau_r) H(\tau - \tau_r) \right] - \\ & - \frac{2}{\tau_s - \tau_r} \left[\varepsilon_y^{(1)*}(\zeta, \tau - \tau_r) H(\tau - \tau_r) - \varepsilon_y^{(1)*}(\zeta, \tau - \tau_s) H(\tau - \tau_s) \right], \quad 0 \leq \zeta \leq 1, \quad \tau \geq 0, \end{aligned} \quad (48)$$

where

$$\varepsilon_y^{(i)*}(\zeta, \tau) = \sum_{n=0}^{\infty} \Lambda^n \varepsilon_n^{(i)*}(\zeta, \tau), \quad 0 \leq \zeta \leq 1, \tau \geq 0, \quad i = 0, 1, \quad (49)$$

$$\varepsilon_n^{(i)*}(\zeta, \tau) = Q_n^{(i)}(\tau) - \zeta R_n^{(i)}(\tau), \quad i = 0, 1, \quad (50)$$

$$Q_n^{(i)}(\tau) = 4I_n^{(i)}(\tau) - 6J_n^{(i)}(\tau), \quad R_n^{(i)}(\tau) = 6I_n^{(i)}(\tau) - 12J_n^{(i)}(\tau), \quad i = 0, 1; n = 0, 1, 2, \dots, \quad (51)$$

$$I_n^{(i)}(\tau) = \int_0^1 T_{c,n}^{(i)*}(\zeta, \tau) d\zeta, \quad J_n^{(i)}(\tau) = \int_0^1 \zeta T_{c,n}^{(i)*}(\zeta, \tau) d\zeta, \quad i = 0, 1; n = 0, 1, 2, \dots, \quad (52)$$

and the dimensionless temperatures $T_c^{(i)*}(\zeta, \tau)$, $i = 0, 1$ has the form (36). Substituting the functions $T_{c,n}^{(i)*}(\zeta, \tau)$, $i = 0, 1; n = 0, 1, 2, \dots$, (38), (39) at the right side of equations (52) and taking into account the value of the integrals:

$$L_0(x) \equiv \int_0^x F_0(t) dt = \frac{1}{4} + \frac{x}{2\sqrt{\pi}} \exp(-x^2) - \frac{(1+2x^2)}{4} \operatorname{erfc}(x), \quad (53)$$

$$M_0(x) \equiv \int_0^x t F_0(t) dt = \frac{1}{6\sqrt{\pi}} - \frac{(1-2x^2)}{6\sqrt{\pi}} \exp(-x^2) - \frac{x^3}{3} \operatorname{erfc}(x), \quad (54)$$

$$L_1(x) \equiv \int_0^x F_1(t) dt = \frac{1}{8} + \frac{x(5+2x^2)}{12\sqrt{\pi}} \exp(-x^2) - \frac{(3+12x^2+4x^4)}{24} \operatorname{erfc}(x), \quad (55)$$

$$M_1(x) \equiv \int_0^x t F_1(t) dt = \frac{1}{15\sqrt{\pi}} - \frac{(1-4x^2-2x^4)}{15\sqrt{\pi}} \exp(-x^2) - \frac{x^3(5+2x^2)}{15} \operatorname{erfc}(x), \quad (56)$$

the following expressions were obtained:

$$I_0^{(i)}(\tau) = 4\tau^{i+1} L_i\left(\frac{1}{2\sqrt{\tau}}\right), \quad I_n^{(i)}(\tau) = 4\tau^{i+1} \left[L_i\left(\frac{2n+1}{2\sqrt{\tau}}\right) - L_i\left(\frac{2n-1}{2\sqrt{\tau}}\right) \right], \quad i = 0, 1; n = 1, 2, 3, \dots, \quad (57)$$

$$J_0^{(i)}(\tau) = 8\tau^{i+3/2} M_i\left(\frac{1}{2\sqrt{\tau}}\right), \quad i = 0, 1, \quad (58)$$

$$J_n^{(i)}(\tau) = 4\tau^{i+1} \left\{ 2\sqrt{\tau} \left[M_i\left(\frac{2n+1}{2\sqrt{\tau}}\right) - 2M_i\left(\frac{n}{\sqrt{\tau}}\right) + M_i\left(\frac{2n-1}{2\sqrt{\tau}}\right) \right] - \right. \\ \left. - 2n \left[L_i\left(\frac{2n+1}{2\sqrt{\tau}}\right) - 2L_i\left(\frac{n}{\sqrt{\tau}}\right) + L_i\left(\frac{2n-1}{2\sqrt{\tau}}\right) \right] \right\}, \quad i = 0, 1; n = 1, 2, 3, \dots \quad (59)$$

It results from formulas (49) and (50) that the dimensionless lateral deformation ε_y^* is linearly dependent on the dimensionless distance ζ from the heated surface of the plate

and that normal stresses σ_y (45) are proportional to the difference of that deformation and the dimensionless temperature $T_c^*(\zeta, \tau)$ (41) or (42).

4. Homogeneous material

The solutions of the corresponding problems of heat conduction for homogeneous semi-space it is possible to obtained from the first component of the expressions (36) and (37) (for $n=0$). Assuming the same thermophysical properties of the foundation and coating ($K_c = K_s = K$, $k_c = k_s = k$) from formulas (22) leads that $\varepsilon = 1$, $\lambda = 0$, $\Lambda = 0$ and then from the expressions (36)-(40) one obtains

$$T^{(0)*}(\zeta, \tau) = 2\sqrt{\tau} \operatorname{ierfc}\left(\frac{\zeta}{2\sqrt{\tau}}\right), \quad 0 \leq \zeta < \infty, \quad \tau \geq 0, \quad (60)$$

$$T^{(1)*}(\zeta, \tau) = \frac{2}{3}\tau\sqrt{\tau} \left\{ 2 \left[1 + \left(\frac{\zeta}{2\sqrt{\tau}} \right)^2 \right] \operatorname{ierfc}\left(\frac{\zeta}{2\sqrt{\tau}}\right) - \left(\frac{\zeta}{2\sqrt{\tau}} \right) \operatorname{erfc}\left(\frac{\zeta}{2\sqrt{\tau}}\right) \right\}, \quad 0 \leq \zeta < \infty, \quad \tau \geq 0. \quad (61)$$

In the present case, the parameter d in formulas (12) can be, for example, the radius of the irradiated zone. Substitution of these solutions (60) and (61) into equations (41) and (42) for $\tau = \tau_s$, gives as a result the dimensionless temperature at the moment when laser is being turned off for the rectangular pulse

$$T^*(\zeta, \tau_s) = T^{(0)*}(\zeta, \tau_s), \quad 0 \leq \zeta < \infty, \quad (62)$$

and for triangular one

$$T^*(\zeta, \tau_s) = \frac{2}{\tau_r} \left[T^{(1)*}(\zeta, \tau_s) - \frac{\tau_s}{\tau_s - \tau_r} T^{(1)*}(\zeta, \tau_s - \tau_r) \right], \quad 0 \leq \zeta < \infty. \quad (63)$$

The final results for the irradiated surface, $\zeta = 0$ in these two cases, have the following known form (Gureev, 1983), respectively

$$T^*(0, \tau_s) = 2\sqrt{\frac{\tau_s}{\pi}}, \quad (64)$$

and

$$T^*(0, \tau_s) = \frac{8}{3}\sqrt{\frac{\tau_s}{\pi}} \left(\frac{\tau_s}{\tau_r} \right) \left(1 - \sqrt{1 - \frac{\tau_r}{\tau_s}} \right). \quad (65)$$

The values of dimensionless lateral stresses σ_y^* corresponding to the temperature fields $T^*(\zeta, \tau)$ (41) or (42) at functions $T^{(i)*}(\zeta, \tau)$, $i=0,1$ (60) and (61) can be obtained from equations (45)-(51) for $n=0$. Taking into account the formulas (53)-(58) the equations (51) leads:

$$Q_0^{(0)}(\tau) = 4\tau \left[1 - 2\sqrt{\frac{\tau}{\pi}} + 2\sqrt{\tau} \operatorname{ierfc}\left(\frac{1}{2\sqrt{\tau}}\right) \right], \quad (66)$$

$$R_0^{(0)}(\tau) = 4\tau \left[\frac{3}{2} - 4\sqrt{\frac{\tau}{\pi}} + \sqrt{\frac{\tau}{\pi}} \exp\left(-\frac{1}{4\tau}\right) + \left(3\sqrt{\tau} - \frac{1}{2\sqrt{\tau}}\right) \operatorname{ierfc}\left(\frac{1}{2\sqrt{\tau}}\right) \right], \quad (67)$$

$$Q_0^{(1)}(\tau) = 4\tau^2 \left[\frac{1}{2} - \frac{4}{5}\sqrt{\frac{\tau}{\pi}} - \frac{1}{5\sqrt{\pi}} \left(\sqrt{\tau} - \frac{1}{6\sqrt{\tau}} \right) \exp\left(-\frac{1}{4\tau}\right) + \left(\sqrt{\tau} - \frac{1}{60\tau\sqrt{\tau}} \right) \operatorname{ierfc}\left(\frac{1}{2\sqrt{\tau}}\right) \right], \quad (68)$$

$$R_0^{(1)}(\tau) = 4\tau^2 \left[\frac{3}{4} - \frac{8}{5}\sqrt{\frac{\tau}{\pi}} + \frac{1}{10\sqrt{\pi}} \left(\sqrt{\tau} + \frac{3}{2\sqrt{\tau}} \right) \exp\left(-\frac{1}{4\tau}\right) + \left(\frac{3}{2}\sqrt{\tau} - \frac{1}{2\sqrt{\tau}} - \frac{3}{40\tau\sqrt{\tau}} \right) \operatorname{ierfc}\left(\frac{1}{2\sqrt{\tau}}\right) \right]. \quad (69)$$

5. Numerical analysis

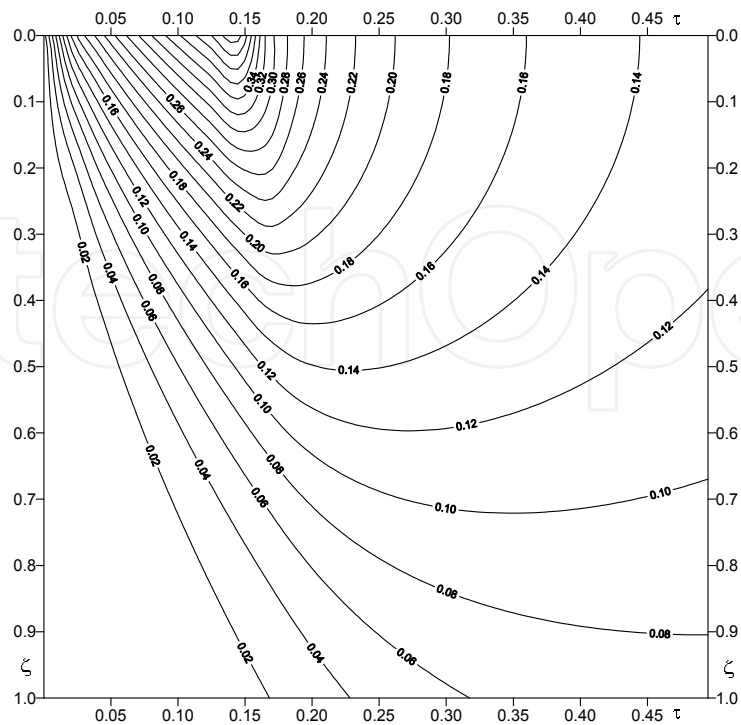
The dimensionless input parameters of the calculations are: spatial coordinate ζ , time (Fourier's criterion) τ , pulse time rise τ_r , duration of the pulse (time of heating) τ_s , ratio of the coefficients of thermal conductivity and thermal diffusivity of the substrate and coating $K^* = K_s / K_c$ and $k^* = k_s / k_c$. Isolines for the dimensionless temperatures $T^* = T / T_0$ and normal stresses $\sigma_y^* = \sigma_y / \sigma_0$ were drawn in the coordinates (ζ, τ) for different temporal profile of the heat pulse. All calculations were conducted for the pulses with dimensionless duration $\tau_s = 0.15$, which is characteristic for irradiation done by CO_2 laser, which emits light at wavelength $10.6 \mu\text{m}$ (Rykalin et al., 1985).

Firstly, the temperature and stress distributions for the case when the coating and the substrate have the same thermophysical and mechanical properties (homogeneous semi-space) will be analysed. Isotherms of the dimensionless temperature T^* at heating by rectangular and triangular, with different rise times, pulses are presented in Figure 2a-d.

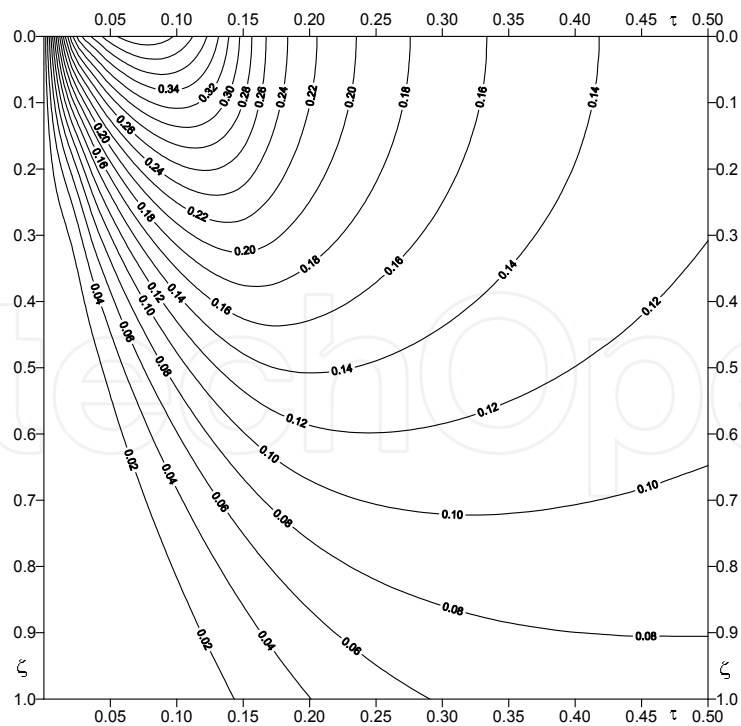
In case of the rectangular pulse the maximum temperature on the surface of the irradiated bulk sample is achieved at the end of the pulse $\tau_s = 0.15$ and its value is $T_{\max}^* = 0.429$ (Fig. 2a). For triangular pulse with different rise times the evolution of temperature proceeds differently – with the increase of back front steepness the moment when the highest temperature is achieved moves closer from the middle of the pulse duration interval (for small values of τ_r) to the moment when laser is switched off τ_s (Fig. 2b-d).

So, for the three considered triangular laser pulses with $\tau_r = 0.001; 0.075; 0.149$ the maximum values of dimensionless temperature are equal $T_{\max}^* = 0.412; 0.475; 0.566$ and are achieved in the moments $\tau = 0.08; 0.10$ and 0.149 , respectively. With increase of the maximal temperature, the effective depth of heating (the depth where the temperature decreases to 5% of its maximum value on the surface) also increases. The presented analysis indicates that the greater value of this depth can be obtained when the laser pulse has the gentle fore front and steep back front.

Isolines for the dimensionless lateral stresses σ_y^* are presented in Figure 3a-d. For heating with the rectangular pulse, in the time interval $0 < \tau \leq 0.15$ the regions of compressive lateral stress ($\sigma_y^* < 0$) occur near the border surfaces $\zeta = 0$ i $\zeta = 1$ (Fig. 3a). Inside this layer tensile stresses are generated ($\sigma_y^* > 0$).



(a)



(b)

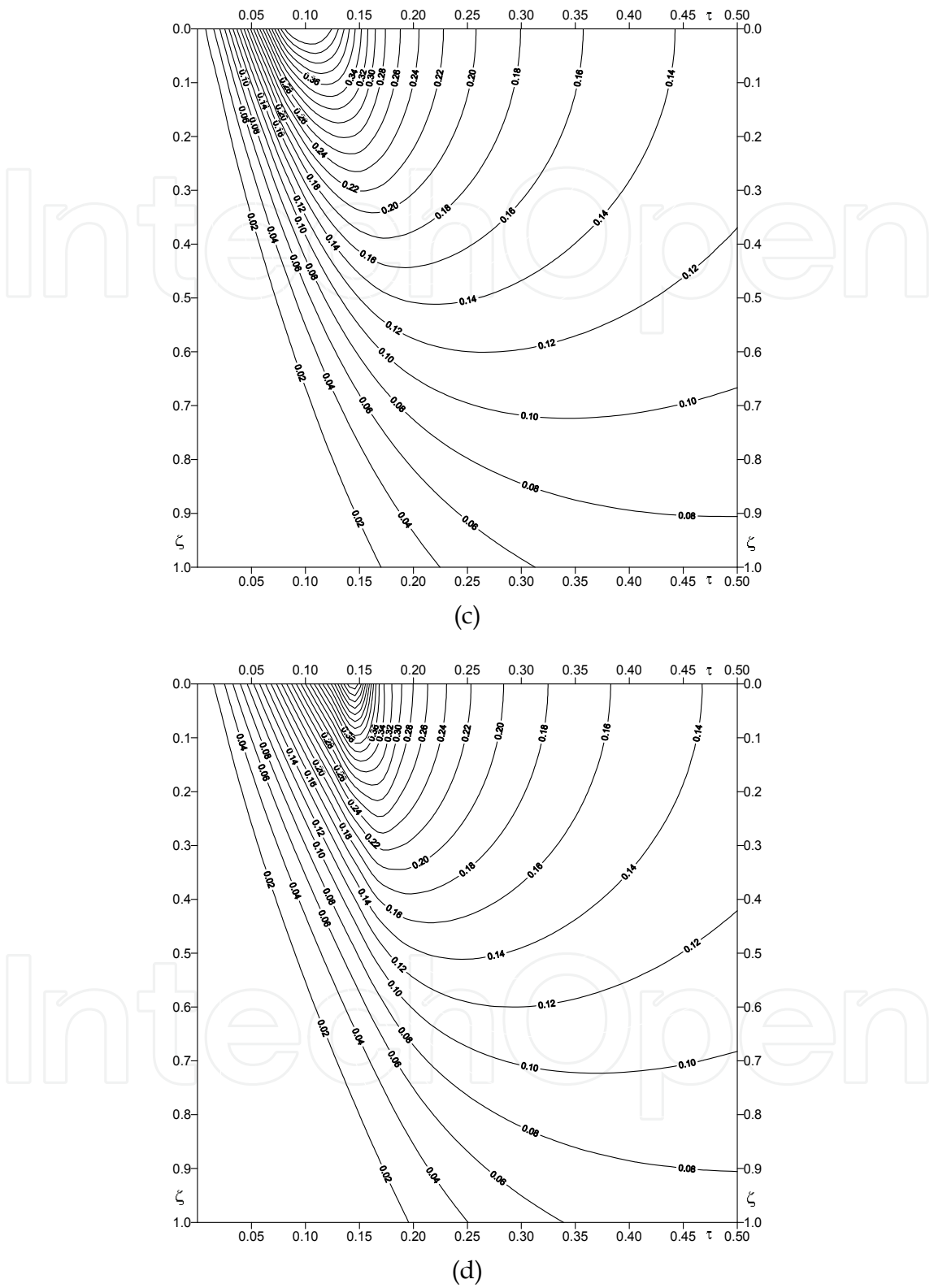
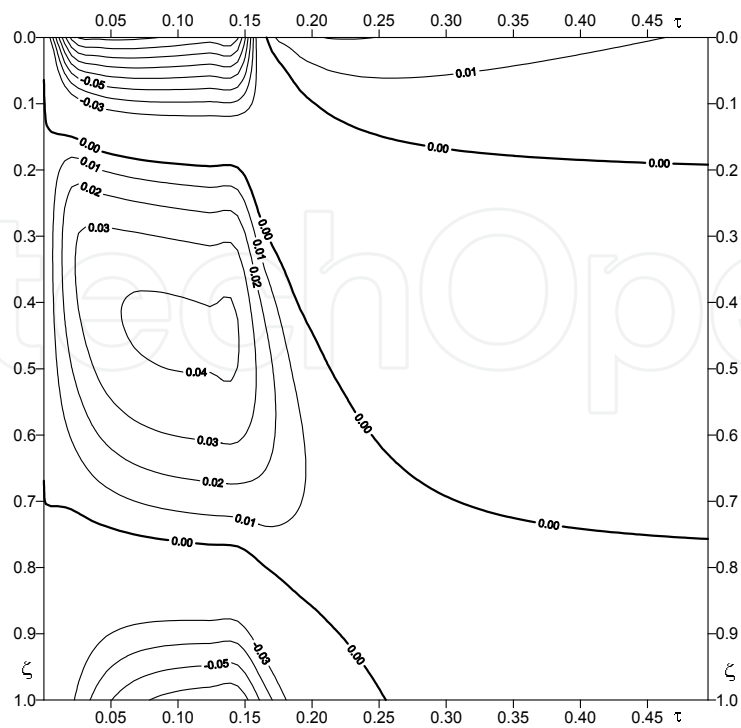
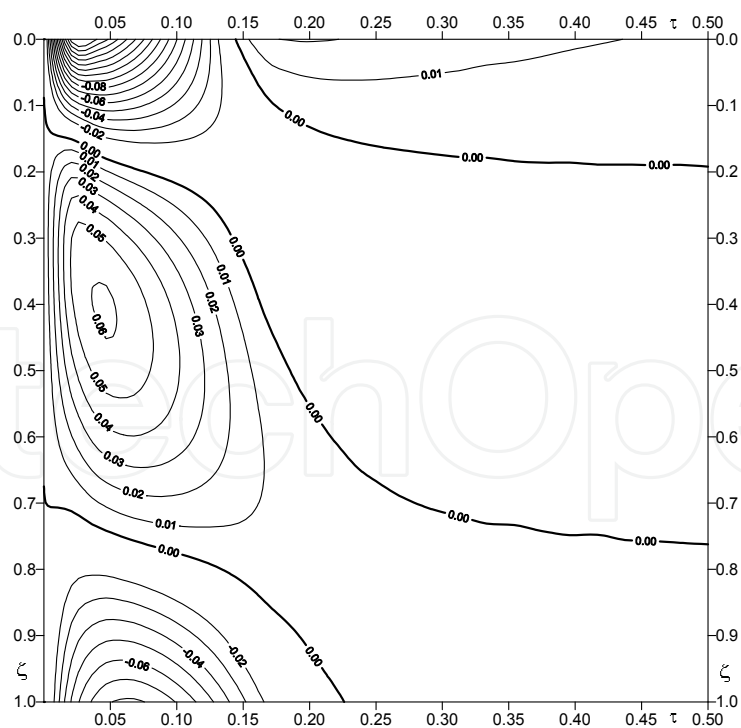


Fig. 2. Isotherms of dimensionless temperature T^* for the dimensionless laser pulse duration $\tau_s = 0.15$: a) rectangular laser pulse; b) c), d) triangular laser pulses for the dimensionless rise time $\tau_r = 0.001$; $\tau_r = 0.075$ and $\tau_r = 0.149$, respectively (Yevtushenko et al., 2007).



(a)



(b)

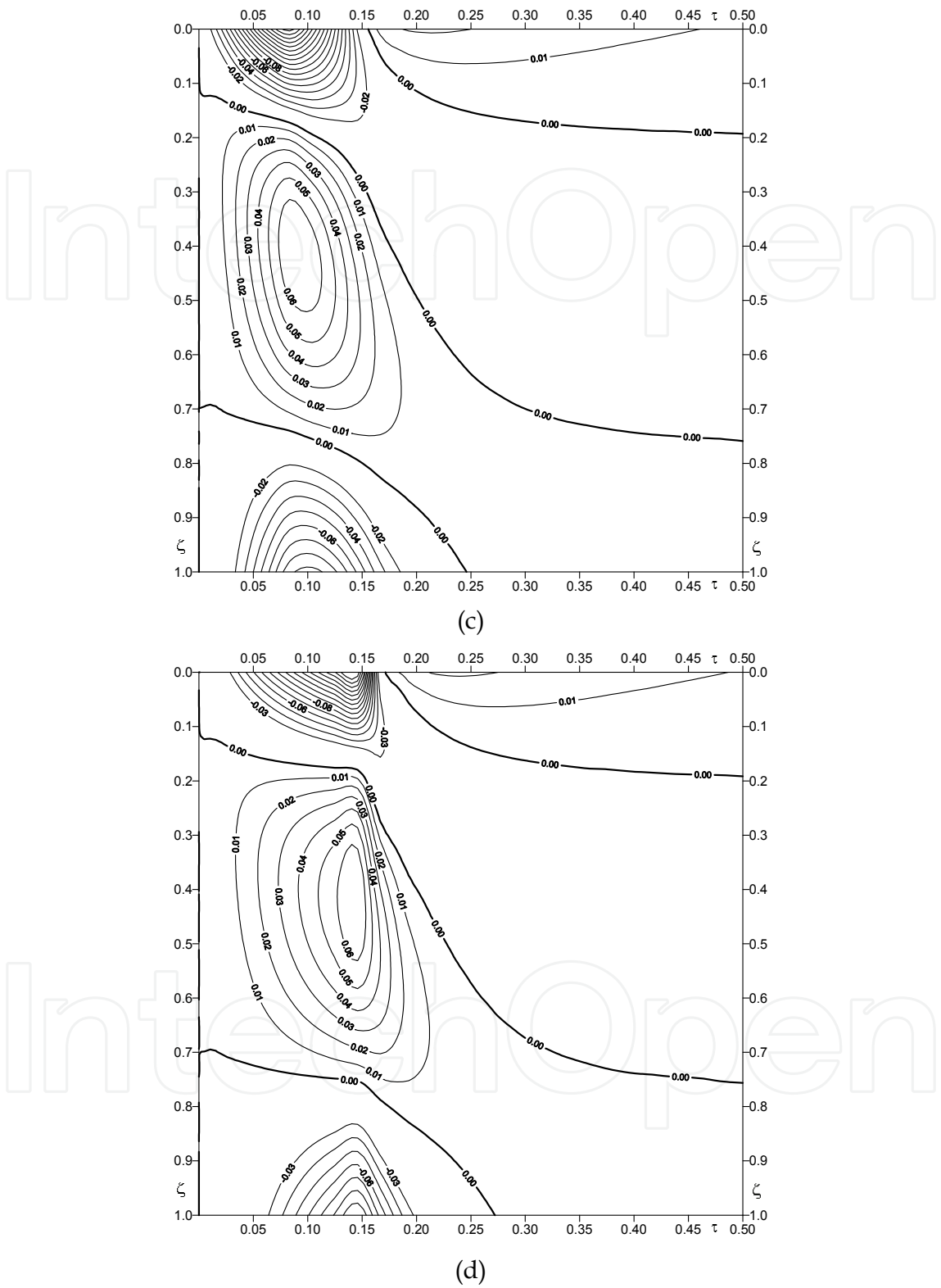


Fig. 3. Isolines of dimensionless lateral stress σ_y^* for the dimensionless laser pulse duration $\tau_s = 0.15$: a) rectangular laser pulse; b) c), d) triangular laser pulses for the dimensionless rise time $\tau_r = 0.001$; $\tau_r = 0.075$ and $\tau_r = 0.149$, respectively (Yevtushenko et al., 2007).

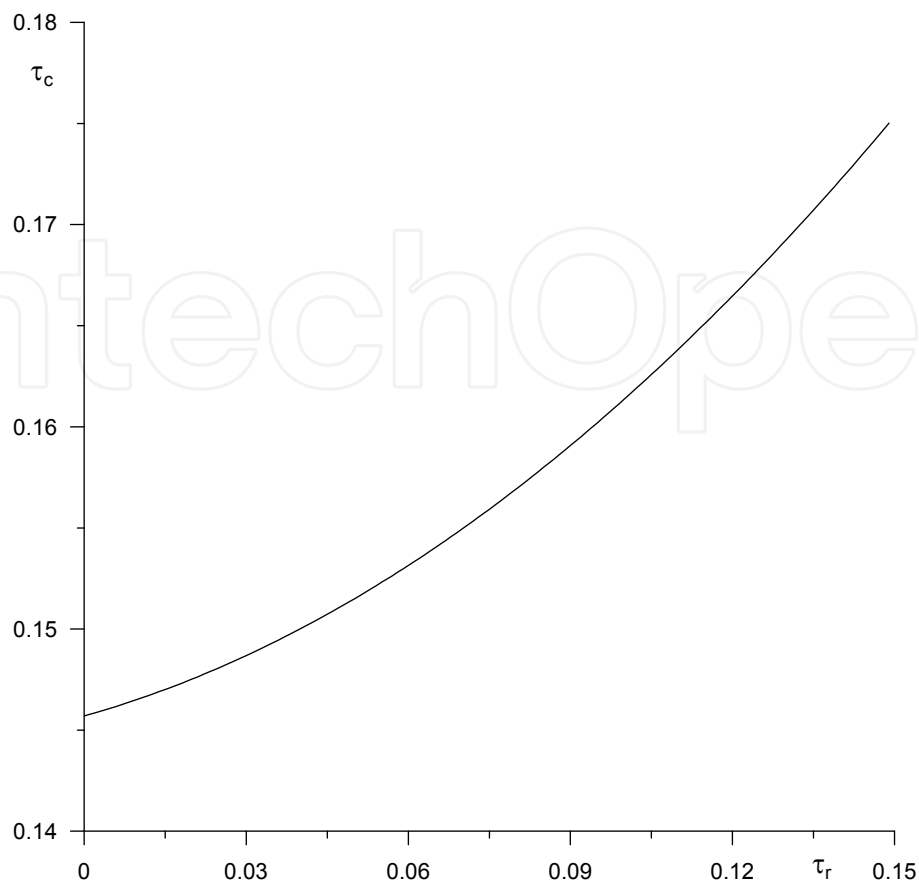


Fig. 4. Dimensionless time τ_c of the sign change of lateral stress σ_y^* on the irradiated surface $\zeta = 0$ versus pulse rise time τ_r for dimensionless time of heating $\tau_s = 0.15$ (Yevtushenko et al., 2007).

Between the regions with compressive and tensile stresses there are two isolines with zero stresses. The third line of zero stresses, which “descends” from the surface $\zeta = 0$, appears when the heating is over ($\tau > 0.15$). It means that during relaxation phase, when there is no more heating, the sign of stresses changes and the region of tensile stresses expands further from the heated surface – the line of zero stresses moves into the plate with the time increase (Fig. 3a).

Somewhat different distribution of dimensionless lateral stress σ_y^* is observed when irradiation is realised with the triangular laser pulses (Fig. 3b-d). In the heating phase ($0 < \tau < 0.15$) compressive superficial stresses occur and the isotherms are much denser near the points of the greatest intensity of the heat flux. For the pulse with steep fore front ($\tau_r = 0.001$) it appears at the very beginning of heating and for the pulse with the steep back front ($\tau_r = 0.149$) – nearly in the moment when the heat source is switched off. The change of stress sign does not necessarily take place after the heat source is off, what was the case for uniform heating.

For the heating with triangular pulse with steep fore front the isoline of zero stresses occurs on the irradiated surface already during the heating phase, before its end (Fig. 3b). The magnitude of tensile stresses during the relaxation phase is more or less the same for the laser pulses of rectangular and triangular shape.

For greater pulse rise times τ_r the dimensionless time τ_c , connected with the change of stresses type from compressive to tensile one also increases (Fig. 4). This dependence is approximately described by the equation $\tau_c = 0.8173\tau_r^2 + 0.075\tau_r + 0.1457$.

In thermal processing of brittle materials, it is the sign change of superficial stresses what plays key role in controlled thermal splitting (Dostanko et al., 2002). The beginning of superficial cracks generation is accompanied with the monotonic increase of tensile lateral stresses and makes the controlled evolution of the crevices possible. By equating the relation (45) to 0 at $\tau = \tau_c > \tau_s$, $\zeta = 0$ and taking into account the equations (42), (48), (49), one obtains:

$$Q_0^{(0)}(\tau_c) - Q_0^{(0)}(\tau_c - \tau_s) = \frac{2}{\sqrt{\pi}}(\sqrt{\tau_c} - \sqrt{\tau_c - \tau_s}), \tag{70}$$

where the function $Q_0^{(0)}(\tau)$ has the form (66). With the absolute inaccuracy, smaller than 3%, the solution of nonlinear equation (70) can be approximated by the function $\tau_c = -1.133\tau_s^3 + 1.172\tau_s^2 + 0.604\tau_s + 0.052$ (Fig. 5).

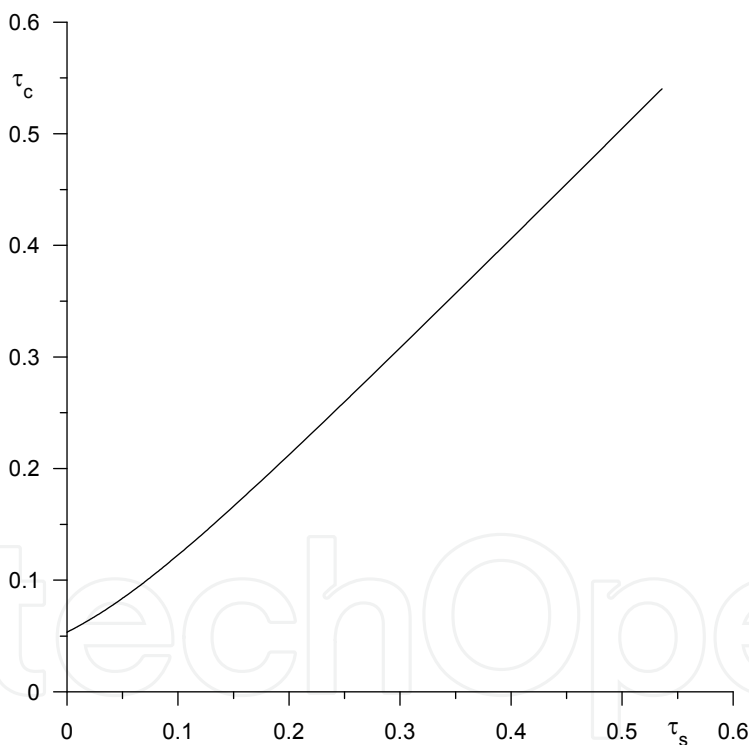


Fig. 5. Dimensionless time τ_c of the sign change of lateral stress σ_y^* on the irradiated surface $\zeta = 0$ versus dimensionless duration τ_s of the rectangular laser pulse (Yevtushenko et al., 2007).

The forced cooling of the surface in the moment time $t = t_c$ would cause the jump of temperature $\Delta T = T(0, t_c - 0) - T(0, t_c + 0)$ in thin superficial layer. From the equations (45) and (46) it follows, that the dimensionless lateral deformation of the plate ε_y^* is determined by the integral characteristic of temperature only. For this reason, the rapid cooling of the thin film, practically, does not change the surface deformation $\varepsilon_y(0, t_c + 0) = \alpha_c T(0, t_c - 0)$ but

at the same moment it produces the increase of the normal stresses $\sigma_y(0, t_c + 0) = \alpha_c \Delta T$. Finally, the development of the superficial crack can be described as a series of the following phases:

1. due to local short heating a surface of the sample in it the field of normal lateral stresses is formed;
2. tensile lateral stresses occur near the subsurface cooled region and are proportional to the temperature jump observed before and after the cooling agent is applied;
3. when the stresses exceeds the tensile strength of the material, the surface undergoes tear;
4. development of the crack into the material is limited by the regions of lateral compressive stress, which occur beneath the cooled surface.

As mentioned in the introduction, there is considerable interest (for scientific and practical reasons) in thermal processing of ceramic coatings from zirconium dioxide ZrO_2 . Authors presented the numerical examinations of thermal stresses distribution for the system consisting of ZrO_2 ceramic coating ($K_c = 2.0 \text{ W/(mK)}$, $k_c = 0.8 \cdot 10^{-6} \text{ m}^2/\text{s}$), deposited on the 40H steel substrate ($K_s = 41.9 \text{ W/(mK)}$, $k_s = 10.2 \cdot 10^{-6} \text{ m}^2/\text{s}$) (Fig. 6). The coefficient of thermal activity for this system is equal $\varepsilon = 5.866$ and the parameter λ found from the equation (22), has the value $\lambda = -0.708$. Thermal diffusivity of zirconium dioxide is small when compared with the value for steel. That difference is the cause of high temperatures on the processed surface and considerably higher than for the homogeneous half-space (one order of magnitude) lateral tensile stresses generated in the superficial layer when the heating is finished. So, the thermal processing of the coating from zirconium dioxide leads to the generation of superficial cracks, which divide the surface into smaller fragments. Of course the distribution of cracks at different depths depends on the heat flux intensity, the diameter of the laser beam, pulse duration and other parameters of the laser system.

But when using dimensionless variables and parameters the results can be compared and the conclusion is that for the heating duration $\tau_s = 0.15$, penetration depth of cracks for coating-substrate system (ZrO_2 -40H steel) is, more than two times greater than for the homogeneous material (one can compare Figs. 3a and 6).

The opposite, to the discussed above, combination of thermo-physical properties of the coating and the substrate is represented by the copper-granite system, often used in ornaments decorating interiors of the buildings like theatres and churches. For the copper coating $K_c = 402 \text{ W/(mK)}$, $k_c = 125 \cdot 10^{-6} \text{ m}^2/\text{s}$, while for the granite substrate $K_s = 1.4 \text{ W/(mK)}$, $k_s = 0.505 \cdot 10^{-6} \text{ m}^2/\text{s}$, what means that the substrate is practically thermal insulator and the coating has good thermal conductivity (see Figs. 7 and 9). The distribution of lateral thermal stresses for copper-granite system is presented in Fig. 8. In this situation, when the thickness of the coating increases, the temperature on the copper surface decreases. Therefore the effective depth of heat penetration into the coating is greater for the better conducting copper than for thermally insulating zirconium dioxide (ZrO_2) (see Figs. 6 and 8). We note that near to the heated surface $\zeta = 0$ lateral stresses σ_y are compressive not only in the heating phase $0 < \tau < 0.15$ but also during relaxation time, when the heat source is off. Considerable lateral tensile stresses occur during the cooling phase close to the interface of the substrate and the coating, $\zeta = 1$. This region of the tensile stresses on the copper-granite interface can destroy their contact and in effect the copper coating exfoliation can result.

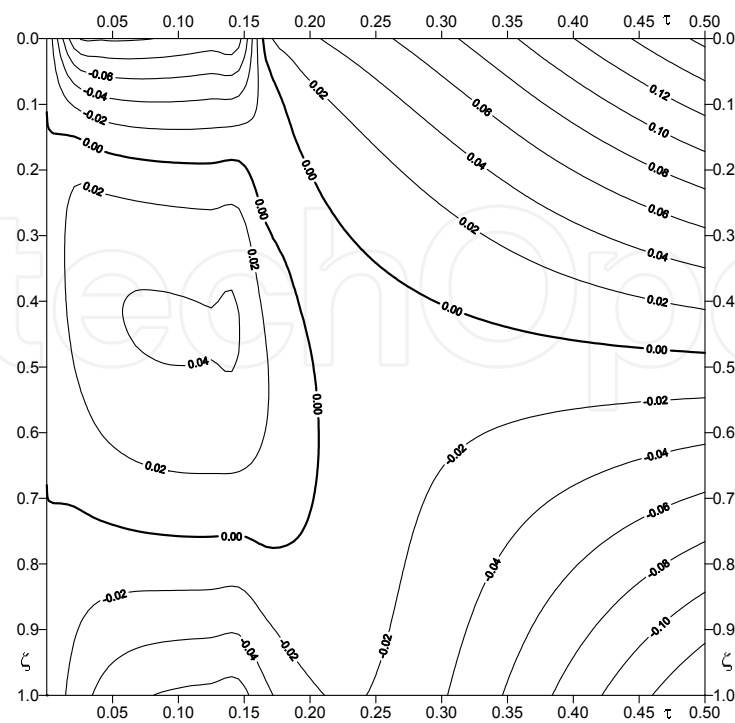


Fig. 6. Isolines of dimensionless lateral stress σ_y^* for ZrO_2 ceramic coating and 40H steel substrate at rectangular laser pulse duration $\tau_s = 0.15$ (Yevtushenko et al., 2007).

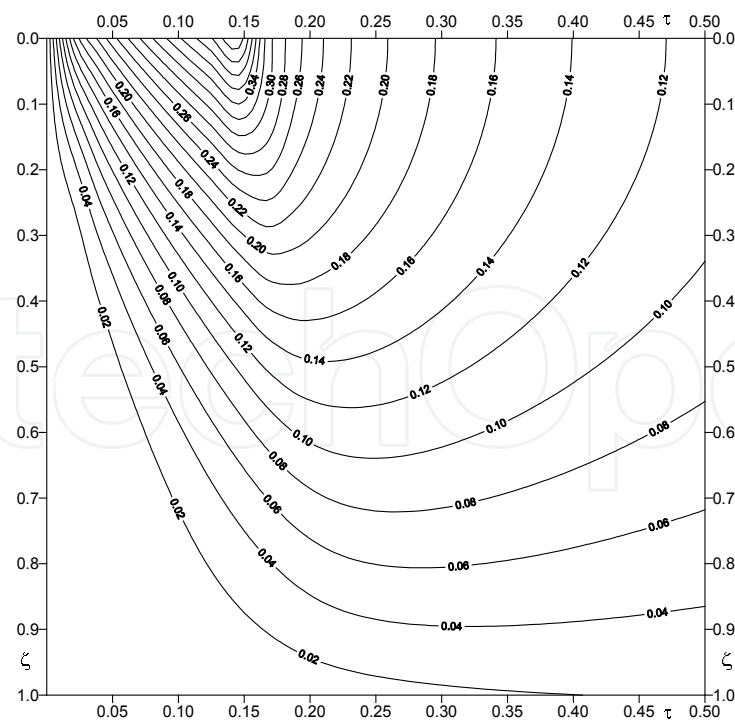


Fig. 7. Isotherms of dimensionless temperature T^* for ZrO_2 ceramic coating and 40H steel substrate at rectangular laser pulse duration $\tau_s = 0.15$ (Yevtushenko et al., 2007).

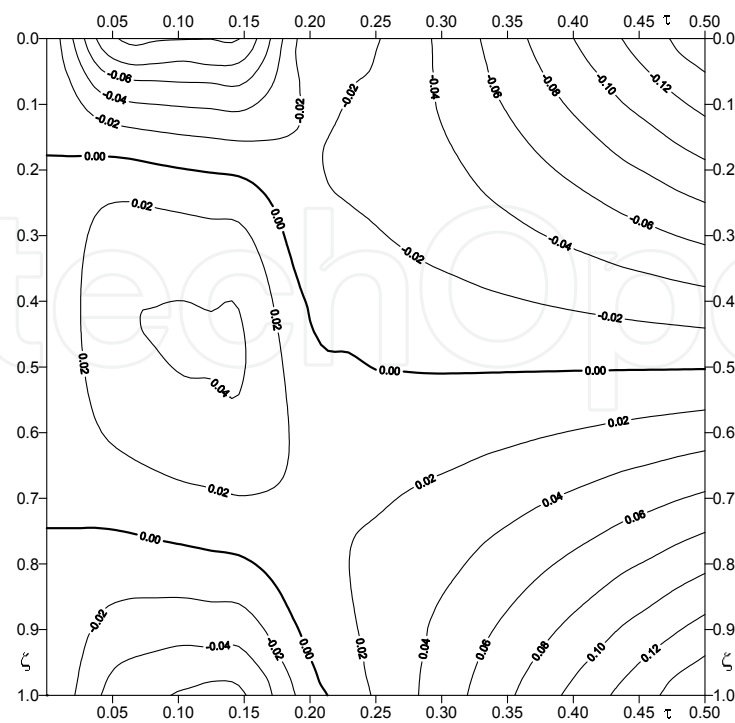


Fig. 8. Isolines of dimensionless lateral stress σ_y^* for copper coating and granite substrate at rectangular laser pulse duration $\tau_s = 0.15$ (Yevtushenko et al., 2007).

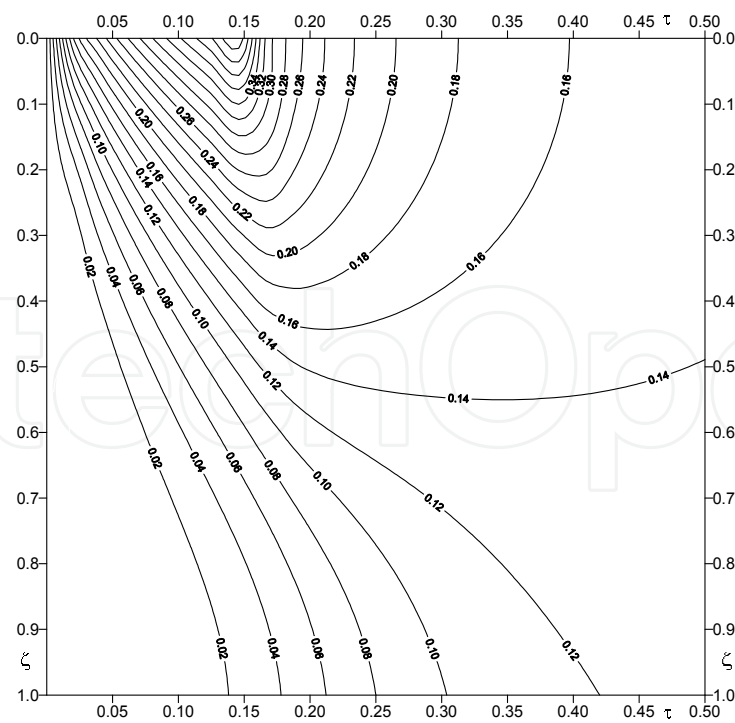


Fig. 9. Isotherms of dimensionless temperature T^* for copper coating and granite substrate at rectangular laser pulse duration $\tau_s = 0.15$ (Yevtushenko et al., 2007).

6. Effective absorption coefficient during laser irradiation

The effective absorption coefficient A in the formula (1) and (12) is defined as the ratio of laser irradiation energy absorbed on the metal's surface and the energy of the incident beam (Rozniakowski, 2001). This dimensionless parameter applies to the absorption on the metal's surface, on the very sample surface (so called "skin effect"). The absorption coefficient A can be found in book (Sala, 1986) or obtained on the basis of calorimetric measurements (Ujihara, 1972). The mixed method of effective absorption coefficient determination for some metals and alloys was presented by Yevtushenko et al., 2005. This method is based on the solution of axisymmetric boundary-value heat conduction problem for semi-space with circular shape line of division in the boundary conditions and on the metallographic measurements of dimensions of laser induced structural changes in metals. The calculations in this method are very complex because, in particular, the numerical calculation of the Hankel's integrals has to be done. Therefore, we shall try to use with this purpose obtained above the analytical solution of the transient one-dimensional heat conduction problem for homogeneous semi-space in the form

$$T(z, t) = AT'_0 T^*(\zeta, \tau), \quad z \geq 0, t \geq 0, \quad (71)$$

where, taking the formula (12) into account, the coefficient $T'_0 = T_0 / A$ and the dimensionless temperature $T^*(\zeta, \tau)$ is defined by formulae (41) and (60). It should be noticed that the temperature on the irradiated surface has maximum value at the moment of laser switching off, for $t = t_s$ ($\tau = \tau_s$), and in the superficial layers the maximum is reached for $t \equiv t_h = t_s + \Delta t$ (in dimensionless units, for $\tau_h = \tau_s + \Delta \tau$, $\Delta \tau = k\Delta t / d^2$, d is the radius of the irradiated zone). The parameter Δt ($\Delta \tau$) is known as "the retardation time" (Rozniakowska & Yevtushenko, 2005). The time interval, when the temperature T reaches its maximum in the point $z = z_h$ beneath the heated surface, can be found from the condition:

$$\frac{\partial T(z_h, t)}{\partial t} = 0, \quad t > t_s > 0. \quad (72)$$

By taking into account the solutions (71), (41) and (60), the equation (72) can be rewritten as:

$$\frac{\partial T^*(\zeta_h, \tau)}{\partial \tau} = \frac{1}{\sqrt{\pi\tau}} \exp\left(-\frac{\zeta_h^2}{4\tau}\right) - \frac{1}{\sqrt{\pi(\tau - \tau_s)}} \exp\left[-\frac{\zeta_h^2}{4(\tau - \tau_s)}\right] = 0, \quad \tau > \tau_s > 0, \quad (73)$$

where $\zeta_h = z_h / d$. After substituting $\tau \equiv \tau_h = \tau_s + \Delta \tau$ in equation (73), one gets

$$\sqrt{\frac{\Delta \tau}{\tau_s + \Delta \tau}} = \exp\left[-\frac{\zeta_h^2 \tau_s}{4\Delta \tau(\tau_s + \Delta \tau)}\right]. \quad (74)$$

From the equation (74) for the known dimensionless hardened layer depth ζ_h and the pulse duration τ_s , the dimensionless retardation time $\Delta \tau$ can be found. On the other hand, at known $\Delta \tau$ from equation (74) we find the dimensionless hardened layer depth ζ_h of maximum temperature can be found:

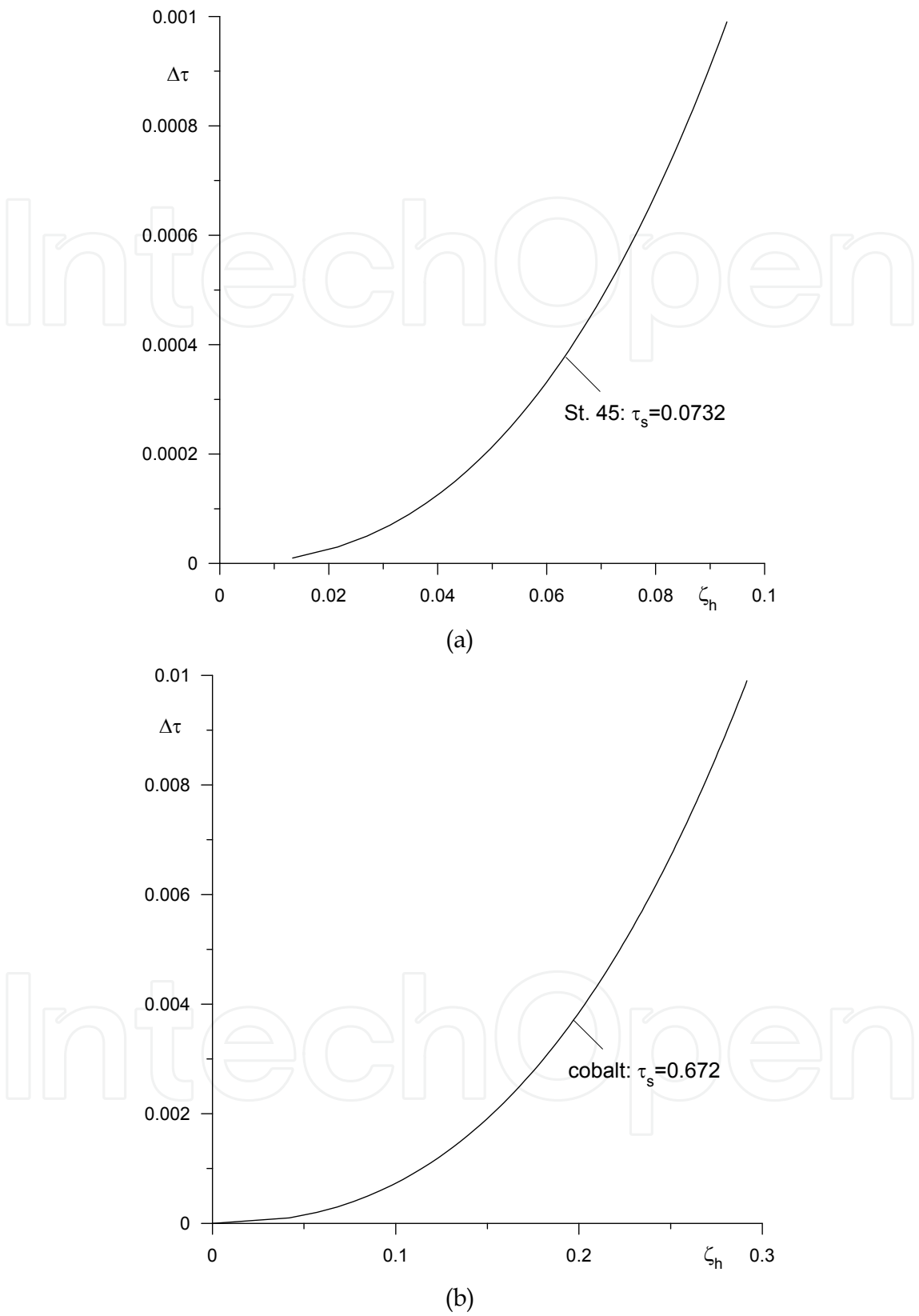


Fig. 10. Dimensionless hardened layer depth ζ_h from the heated surface versus dimensionless retardation time $\Delta\tau$, for the dimensionless laser pulse duration: a) $\tau_s = 0.0732$ (St.45 steel sample); b) $\tau_s = 0.672$ (Co monocrystal sample) (Yevtushenko et al., 2005).

parameter metal	laser type	d mm	t_s ms	$q_0 \times 10^{-9}$ W/m ²	K Wm ⁻¹ K ⁻¹	$k \times 10^5$ m ² s ⁻¹	T_h K	z_h μm
St. 45	Nd:YAG	0.64	2	0.58	33.5	1.5	1123	40
Co	QUANTUM15	0.35	4.5	4.62	70.9	1.83	693	100

Table 1. Input data needed for the calculations of the effective absorption coefficients for the St.45 steel and Co monocrystal samples.

$$\zeta_h = \sqrt{2\Delta\tau \left(1 + \frac{\Delta\tau}{\tau_s}\right) \ln \left(1 + \frac{\tau_s}{\Delta\tau}\right)}.$$

(75)

The curves which represent the dependency of ζ_h on the parameter $\Delta\tau$, for fixed values $\tau_s = 0.0732$ and $\tau_s = 0.672$ are shown in Figs. 10a and 10b, respectively. The dimensionless retardation time quickly increases with the distance increase from the heated surface. The dimensionless pulse durations τ_s were calculated from equation (12) with the use of material constants characteristic for St. 45 steel and Co monocrystals (Table 1), which were presented by Yevtushenko et al., 2005.

Assuming the temperature T_h of the structural phase transition, characteristic for the material, is achieved to a depth z_h from the heated surface at the moment t_h . It should be noticed that for steel the region of structural phase transitions is just the hardened layer, while for cobalt – it is the region where, as a result of laser irradiation, no open domains of Kittel’s type are observed.

It can be assumed that the thickness of these layers z_h , is known – it can be found in the way described by Rozniakowski, 2001. Then, from the condition

$$T(z_h, t_h) = T_h,$$

(76)

the following formula, which can be used for the determination of the effective absorption coefficient, is obtained:

$$A = \frac{T_h}{T'_0} \left[T^*(\zeta_h, \tau_h) \right]^{-1},$$

(77)

where dimensionless temperature T^* is expressed by equations (41) and (60), the dimensionless retardation time $\Delta\tau$ can be found from the equation (75) and the constant $T'_0 = q_0 d / K$. The input data needed for the calculations by formula (77) are included in Table 1. Experimental results obtained by Rozniakowski, 1991, 2001 as well as the solutions for the axisymmetric (Yevtushenko et al., 2005) and one-dimensional model are presented in

<div>parameter</div> <div>metal</div>	$T_0' \times 10^{-5},$ K^{-1}	$\zeta_h,$ -	$\tau_s,$ -	$\Delta \tau \times 10^3$ -	A exp.	A axisym.	A one-dimen.
St. 45	0.111	0.0625	0.0732	0.36	0.3 ÷ 0.5	0.42	0.41
Co	0.228	0.286	0.672	9.8	0.1	0.112	0.045

Table 2. Values of the effective absorption coefficient for the St.45 steel and Co monocrystal samples.

Values of the effective absorption coefficient for the St.45 steel sample irradiated with pulses of short duration $\tau_s = 0.0732$, found on the basis of the solutions for axisymmetric ($A = 0.42$) and one-dimensional ($A = 0.41$) transient heat conduction problem are nearly the same, and correspond to the middle of the experimentally obtained values range $A = 0.3 \div 0.5$ (Table 2). The cobalt monocrystal samples were irradiated with pulses of much longer duration $\tau_s = 0.672$. In this case, there is more than twofold difference of A values found on the basis of the solutions for axisymmetric ($A = 0.112$) and one-dimensional ($A = 0.045$) transient heat conduction problem. Moreover, only the value of effective absorption coefficient obtained from the axisymmetric solution of transient heat conduction problem corresponds to the experimental value $A = 0.1$. In that manner, it was proved that the solution of one-dimensional boundary heat conduction problem of parabolic type for the semi-space can be successfully applied in calculations of the effective absorption coefficient only for laser pulses of dimensionless short duration $\tau_s \ll 1$. Otherwise, the solution of axisymmetric heat conduction problem must be used.

7. Conclusions

The analytical solution of transient boundary-value heat conduction problem of parabolic type was obtained for the non-homogeneous body consisting of bulk substrate and a thin coating of different material deposited on its surface. The heating of the outer surface of this coating was realised with laser pulses of the rectangular or triangular time structure. The dependence of temperature distribution in such body on the time parameters of the pulses was examined. It was proved that the most effective, from the point of view of the minimal energy losses in reaching the maximal temperature, is irradiation by pulses of the triangular form with flat forward and abrupt back front. Analysis of the evolution of stresses in the homogeneous plate proves that when it is heated, considerable lateral compressive stresses occur near the outer surface. The value of this stresses decreases when the heating is stopped and after some time the sign changes – what means that the tensile stresses takes place. The time when it happens increases monotonously with increase of a thermal pulse duration (for rectangular laser pulses) or with increase of rise time (for triangular laser pulses). When the lateral tensile stresses exceed the strength of the material then a crack on the surface can arise. The region of lateral compressive stresses, which occur beneath the surface, limits their development into the material.

The presence of the coating (for example, ZrO_2) with thermal conductivity lower than for the substrate results in considerably higher than for the homogeneous material, lateral tensile stresses in the subsurface after the termination of heating. The depth of thermal splitting is also increased in this case. When the material of the coating (for example, copper) has greater conductivity than the substrate (granite) then the stresses have compressive character all the time. The coating of this kind can protect from thermal splitting. The region that is vulnerable for damage in this case is close to the interface of the substrate and the coating, where considerable tensile stresses occur during the cooling phase.

The method for calculation of the effective absorption coefficient during high-power laser irradiation based on the solution of one-dimensional boundary problem of heat conduction for semi-space, when heating is realised with short pulses, was proposed, too.

8. References

- Coutouly, J. F. et al. (1999). Laser diode processing for reducing core-loss of gain-oriented silicon steels, *Lasers Eng.*, Vol. 8, pp. 145-157.
- Dostanko, A. P. et al. (2002). *Technology and technique of precise laser modification of solid-state structures*, Tiechnoprint, Minsk (in Russian).
- Duley, W. W. (1976). *CO₂ Lasers: Effects and Applications*, Acad. Press, New York.
- Gureev, D. M. (1983). Influence of laser pulse shape on hardened coating depth, *Kvant Elektron* (in Russian), Vol. 13, No. 8, pp. 1716-1718.
- Hector, L. G. & Hetnarski, R. B. (1996). Thermal stresses in materials due to laser heating, In: R. B. Hetnarski, *Thermal Stresses IV*, pp. 1-79, North-Holland.
- Kim, W. S. et al. (1997). Thermoelastic stresses in a bonded coating due to repetitively pulsed laser radiation, *Acta Mech.*, Vol. 125, pp. 107-128.
- Li, J. et al. (1997). Decreasing the core loss of grain-oriented silicon steel by laser processing, *J. Mater. Process. Tech.*, Vol. 69, pp. 180-185.
- Loze, M. K. & Wright, C. D. (1997). Temperature distributions in a semi-infinite and finite-thickness media as a result of absorption of laser light, *Appl. Opt.*, Vol. 36, pp. 494-507.
- Luikov, A. V. (1986). *Analytical Heat Diffusion Theory*, Academic Press, New York.
- Ready, J. F. (1971). *Effects of high-power laser radiation*, Academic Press, New York.
- Rozniakowska, M. & Yevtushenko, A. A. (2005). Influence of laser pulse shape both on temperature profile and hardened coating depth, *Heat Mass Trans.*, Vol. 42, pp. 64-70.
- Rozniakowski, K. (1991). Laser-excited magnetic change in cobalt monocrystal, *J. Materials Science*, Vol. 26, pp. 5811-5814.
- Rozniakowski, K. (2001). *Application of laser radiation for examination and modification of building materials properties*, (in Polish), BIGRAF, Warsaw.
- Rykalin, N. N. et al. (1985). *Laser and electron-radiation processing of materials*, (in Russian), Mashinostroenie, Moscow.
- Said-Galiyev, E. E. & Nikitin, L. N. (1993). Possibilities of Modifying the Surface of Polymeric Composites by Laser Irradiation, *Mech. Comp. Mater.*, Vol. 29, pp. 259-266.
- Sala, A. (1986). *Radiant properties of materials*, Elsevier, Amsterdam.

- Sheng, P. & Chryssolouris, G. (1995). Theoretical Model of Laser Grooving for Composite Materials, *J. Comp. Mater.*, Vol. 29, pp. 96-112.
- Timoshenko, S. P. & Goodier, J. N. (1951). *Theory of Elasticity*, McGraw-Hill, New York.
- Ujihara, K. (1972). Reflectivity of metals at high temperatures, *J. Appl. Phys.*, Vol. 43, pp. 2376-2383.
- Welch, A. J. & Van Gemert, M. J. C. (1995). *Optical-thermal response of laser-irradiated tissue*, Plenum Press, New York and London.
- Yevtushenko, A. A. et al. (2005). Evaluation of effective absorption coefficient during laser irradiation using of metals martensite transformation, *Heat Mass Trans.*, Vol. 41, pp. 338-346.
- Yevtushenko, A.A. et al. (2007). Laser-induced thermal splitting in homogeneous body with coating, *Numerical Heat Transfer, Part A.*, Vol. 52, pp. 357-375.

IntechOpen



Laser Pulse Phenomena and Applications

Edited by Dr. F. J. Duarte

ISBN 978-953-307-405-4

Hard cover, 474 pages

Publisher InTech

Published online 30, November, 2010

Published in print edition November, 2010

Pulsed lasers are available in the gas, liquid, and the solid state. These lasers are also enormously versatile in their output characteristics yielding emission from very large energy pulses to very high peak-power pulses. Pulsed lasers are equally versatile in their spectral characteristics. This volume includes an impressive array of current research on pulsed laser phenomena and applications. *Laser Pulse Phenomena and Applications* covers a wide range of topics from laser powered orbital launchers, and laser rocket engines, to laser-matter interactions, detector and sensor laser technology, laser ablation, and biological applications.

How to reference

In order to correctly reference this scholarly work, feel free to copy and paste the following:

Aleksander Yevtushenko and Malgorzata Rozniakowska-Klosinska (2010). The Effect of the Time Structure of Laser Pulse on Temperature Distribution and Thermal Stresses in Homogeneous Body with Coating, *Laser Pulse Phenomena and Applications*, Dr. F. J. Duarte (Ed.), ISBN: 978-953-307-405-4, InTech, Available from: <http://www.intechopen.com/books/laser-pulse-phenomena-and-applications/the-effect-of-the-time-structure-of-laser-pulse-on-temperature-distribution-and-thermal-stresses-in->

INTECH
open science | open minds

InTech Europe

University Campus STeP Ri
Slavka Krautzeka 83/A
51000 Rijeka, Croatia
Phone: +385 (51) 770 447
Fax: +385 (51) 686 166
www.intechopen.com

InTech China

Unit 405, Office Block, Hotel Equatorial Shanghai
No.65, Yan An Road (West), Shanghai, 200040, China
中国上海市延安西路65号上海国际贵都大饭店办公楼405单元
Phone: +86-21-62489820
Fax: +86-21-62489821

© 2010 The Author(s). Licensee IntechOpen. This chapter is distributed under the terms of the [Creative Commons Attribution-NonCommercial-ShareAlike-3.0 License](https://creativecommons.org/licenses/by-nc-sa/3.0/), which permits use, distribution and reproduction for non-commercial purposes, provided the original is properly cited and derivative works building on this content are distributed under the same license.

IntechOpen

IntechOpen